


# Characterization and synthetic biology elements of nonmodel bacteria, *Acetobacteraceae*

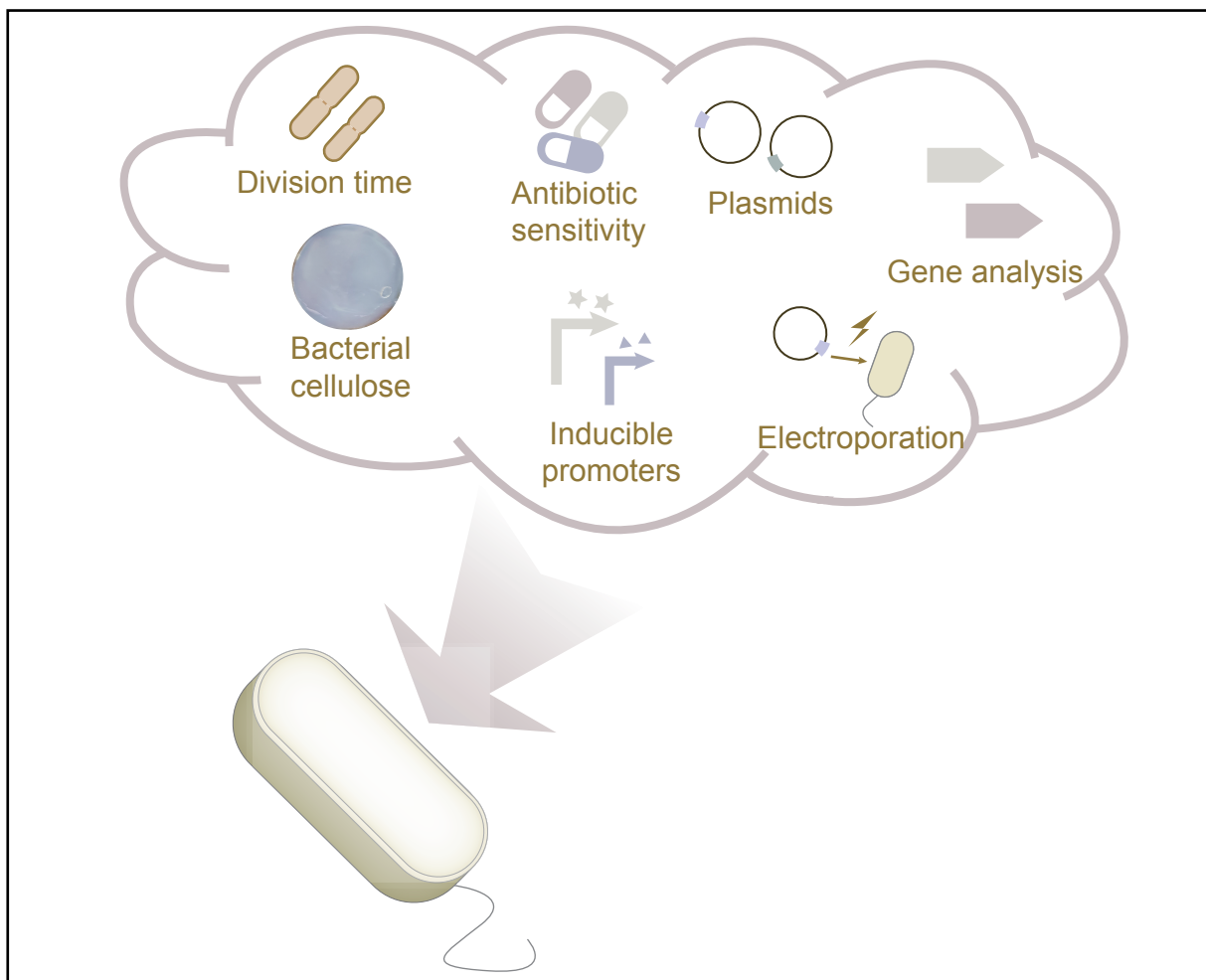
Yanmei Gao 

Province Hefei National Laboratory for Physical Sciences at the Microscale, University of Science and Technology of China, Hefei 230026, China

 Correspondence: Yanmei Gao, E-mail: [ymg@mail.ustc.edu.cn](mailto:ymg@mail.ustc.edu.cn)

© 2024 The Author(s). This is an open access article under the CC BY-NC-ND 4.0 license (<http://creativecommons.org/licenses/by-nc-nd/4.0/>).

## Graphical abstract



Characterization and synthetic biology element of *Acetobacteraceae*.


## Public summary

- The basic properties of three *Acetobacteraceae* strains were analyzed.
- Two inducible promoters were characterized within the three strains, along with the identification of four essential genes for bacterial cellulose production in the *Gluconacetobacter hansenii* ATCC 5358 strain.

# Characterization and synthetic biology elements of nonmodel bacteria, *Acetobacteraceae*

Yanmei Gao 

Province Hefei National Laboratory for Physical Sciences at the Microscale, University of Science and Technology of China, Hefei 230026, China

 Correspondence: Yanmei Gao, E-mail: [ymg@mail.ustc.edu.cn](mailto:ymg@mail.ustc.edu.cn)

© 2024 The Author(s). This is an open access article under the CC BY-NC-ND 4.0 license (<http://creativecommons.org/licenses/by-nc-nd/4.0/>).



Cite This: *JUSTC*, 2024, 54(9): 0907 (13pp)



Read Online

**Abstract:** *Acetobacteraceae* has garnered significant attention because of its unique properties and the broad applications of the bacterial cellulose it produces. However, unlike model strains, *Acetobacteraceae* have few synthetic biology applications because they are difficult to manipulate genetically and have insufficient genetic regulatory elements, among other factors. To address this limitation, this study characterized the fundamental properties and synthetic biology elements of three commonly used bacterial cellulose-producing strains. First, the basic characteristics of the three strains, including their cellulose film production ability, division time, antibiotic susceptibility, and plasmid features, were analyzed. Two inducible promoters (pTrc and pLux101) were subsequently characterized within the three strains. The inducibility of the pTrc promoter was relatively low across the three strains (induction ratio: 1.98–6.39), whereas the pLux101 promoter demonstrated a significantly greater level of inducibility within the three strains (induction ratio: 87.28–216.71). Finally, through gene knockout experiments, this study identified four genes essential for bacterial cellulose film production in the genome of the *Gluconacetobacter hansenii* ATCC 5358 strain. This study not only enriches the library of synthetic biology elements in nonmodel strains, but also lays the foundation for the synthetic biology applications of *Acetobacteraceae*.

**Keywords:** synthetic biology; *Acetobacteraceae*; bacterial cellulose; inducible promoter; nonmodel bacteria

**CLC number:** Q789

**Document code:** A

## 1 Introduction

Synthetic biology has opened new opportunities and challenges in designing bacterial functions and using them in industry, medical treatments, and other fields<sup>[1–3]</sup>. The vast libraries of synthetic biology components within model organisms, such as *Escherichia coli*, *Bacillus subtilis*, and *Saccharomyces cerevisiae*, enable researchers to swiftly obtain custom-engineered strains<sup>[4–6]</sup>. The application of engineered bacteria represents a new biotechnology trend in industrial development and promotes the upgrading and transformation of traditional industries. However, with increasing application demands, researchers have gradually recognized that the inherent limitations in the molecular/physiological characteristics of model organisms restrict their suitability for a wide range of biotechnological tasks<sup>[4,5]</sup>. Therefore, harnessing the innate capabilities of host strains is crucial for achieving specific outcomes in engineered strains<sup>[5–8]</sup>. Consequently, the development and application of nonmodel strains are highly important for the advancement of synthetic biology<sup>[9,10]</sup>.

*Acetobacteraceae*, a widely distributed Gram-negative bacteria, has gained significant attention as a nonmodel strain in recent years<sup>[11–14]</sup>. Owing to its unique oxidative fermentation metabolism, *Acetobacteraceae* plays a crucial role in producing vinegar and fermented beverages<sup>[15,16]</sup>. Additionally, *Acetobacteraceae* is a representative bacteria for producing

bacterial cellulose (BC) and is frequently utilized for the research and mass production of BC films. BC films are renowned for their excellent biocompatibility, breathability, water absorption, and mechanical strength<sup>[17–21]</sup> and have a wide range of applications in fields such as medicine, paper, and textiles. Currently, researchers have conducted in-depth genomic studies on *Acetobacteraceae* strains and characterized some commonly used synthetic biology elements<sup>[22–27]</sup>. However, given the current demand, these studies are still insufficient.

In this study, the division time and BC production capacity of three strains with known genome sequences, *Gluconacetobacter hansenii* ATCC 53582, *Gluconacetobacter xylinus* 700178, and *Komagataeibacter rhaeticus* iGEM, were first analyzed and characterized. The origin of replication (ori) and the stability of replicable plasmids within the three strains were subsequently investigated, and the plasmid transformation efficiency and frequency within these strains were assessed. Additionally, the induction conditions and curves of two inducible promoters, pTrc and pLux101, within the three strains were detailed. Finally, essential genes responsible for BC production in the genome of *G. hansenii* ATCC 53582 were successfully screened and confirmed. This comprehensive study provides a solid foundation for future research and the regulation of *Acetobacteraceae* behavior, particularly in the control of BC film formation.

## 2 Materials and methods

### 2.1 Bacterial strains and culture

The strains and plasmids used in this study are listed in Tables 1 and 2. *Gluconacetobacter hansenii* ATCC 53582 was preserved in our laboratory, whereas *Gluconacetobacter xylinus* 700178 and *Komagataeibacter rhaeticus* iGEM were generously gifted by Siqian Chen (Dongguan University of Technology) and Tom Ellis (Imperial College London), respectively.

ively.

The plasmids used in the experiment were constructed via Gibson assembly and were confirmed to be accurate through sequencing before their transformation into *Acetobacteraceae* strains via electroporation. The success of plasmid transformation and the accuracy of the engineered bacteria were validated through PCR and DNA sequencing.

For plasmid construction and preservation, *Escherichia coli* Top10 was used. *E. coli* was cultured on LB agar or broth at 37 °C, stationary, or at 230 r/min. The *Acetobacteraceae*

**Table 1.** Strains used in this study.

Strain	Describe	Source
<b><i>E. coli</i> strain</b>		
Top10	F <sup>-</sup> , mcrA, (mrr, hsdRMS-mcrBC), 80lacZ M15 lacX74, recA1, araD139, (ara-leu)7697, galU, galK, rpsL(StrR), endA1, nupG	Lab collection
<b><i>Acetobacteraceae</i> strain</b>		
<i>Gluconacetobacter hansenii</i> ATCC 53582	Wild type	Lab collection
<i>Gluconacetobacter xylinus</i> 700178	Wild type	Siqian Chen
<i>Komagataeibacter rhaeticus</i> iGEM	Wild type	Tom Ellis
ΔAB1	<i>G. hansenii</i> ATCC 53582 strain with <i>acsAB1</i> gene knockout, Cm <sup>R</sup>	This study
ΔAB2	<i>G. hansenii</i> ATCC 53582 strain with <i>acsAB2</i> gene knockout, Gm <sup>R</sup>	This study
ΔAB3	<i>G. hansenii</i> ATCC 53582 strain with <i>acsAB3</i> gene knockout, Gm <sup>R</sup>	This study
ΔC1	<i>G. hansenii</i> ATCC 53582 strain with <i>acsC1</i> gene knockout, Cm <sup>R</sup>	This study
ΔC2	<i>G. hansenii</i> ATCC 53582 strain with <i>acsC2</i> gene knockout, Gm <sup>R</sup>	This study
ΔC3	<i>G. hansenii</i> ATCC 53582 strain with <i>acsC3</i> gene knockout, Gm <sup>R</sup>	This study
Δccp	<i>G. hansenii</i> ATCC 53582 strain with <i>ccpAX</i> gene knockout, Cm <sup>R</sup>	This study
Δdgc1	<i>G. hansenii</i> ATCC 53582 strain with <i>dgc1</i> gene knockout, Cm <sup>R</sup>	This study
Δdgc2	<i>G. hansenii</i> ATCC 53582 strain with <i>dgc2</i> gene knockout, Cm <sup>R</sup>	This study
H-plux	<i>G. hansenii</i> ATCC 53582, pLux101-mRFP1-pSEVA331a, Cm <sup>R</sup>	This study
H-mcs	<i>G. hansenii</i> ATCC 53582, pRedawn-MCS-pSEVA331a, Cm <sup>R</sup>	This study
H-trc	<i>G. hansenii</i> ATCC 53582, pTrc-mRFP1-pSEVA331a, Cm <sup>R</sup>	This study
H-9trc	<i>G. hansenii</i> ATCC 53582, pTrc-B009GT-mRFP1-pSEVA331a, Cm <sup>R</sup>	This study
R-plux	<i>K. rhaeticus</i> iGEM, pLux101-mRFP1-pSEVA331a, Cm <sup>R</sup>	This study
R-mcs	<i>K. rhaeticus</i> iGEM, pRedawn-MCS-pSEVA331a, Cm <sup>R</sup>	This study
R-trc	<i>K. rhaeticus</i> iGEM, pTrc-mRFP1-pSEVA331a, Cm <sup>R</sup>	This study
R-9trc	<i>K. rhaeticus</i> iGEM, pTrc-B009GT-mRFP1-pSEVA331a, Cm <sup>R</sup>	This study
X-trc	<i>G. xylinus</i> 700178, pTrc-mRFP1-pSEVA331a, Cm <sup>R</sup>	This study
X-9trc	<i>G. xylinus</i> 700178, pTrc-B009GT-mRFP1-pSEVA331a, Cm <sup>R</sup>	This study
H-PSE	<i>G. hansenii</i> ATCC 53582, J23100-mRFP1-pSEVA331a, Cm <sup>R</sup>	This study
H-MV	<i>G. hansenii</i> ATCC 53582, J23100-mRFP1-pCIMV, Cm <sup>R</sup>	This study
H-PSC	<i>G. hansenii</i> ATCC 53582, J23100-mRFP1-pCIPSC, Cm <sup>R</sup>	This study
H-crep	<i>G. hansenii</i> ATCC 53582, J23100-mRFP1-pCIrep, Cm <sup>R</sup>	This study
H-P15a	<i>G. hansenii</i> ATCC 53582, J23100-mRFP1-pCIP15a, Cm <sup>R</sup>	This study
R-PSE	<i>K. rhaeticus</i> iGEM, J23100-mRFP1-pSEVA331a, Cm <sup>R</sup>	This study
R-MV	<i>K. rhaeticus</i> iGEM, J23100-mRFP1-pCIMV, Cm <sup>R</sup>	This study
X-PSE	<i>G. xylinus</i> 700178, J23100-mRFP1-pSEVA331a, Cm <sup>R</sup>	This study
X-MV	<i>G. xylinus</i> 700178, J23100-mRFP1-pCIMV, Cm <sup>R</sup>	This study
X-crep	<i>G. xylinus</i> 700178, J23100-mRFP1-pCIrep, Cm <sup>R</sup>	This study

Cm<sup>R</sup> and Gm<sup>R</sup> indicate the expression of chloramphenicol and gentamicin resistance genes, respectively.

**Table 2.** Plasmids used in this study.

Plasmid	Ori	Feature
pSEVA331a	pBBR1	Empty vector, Cm <sup>r</sup>
J23100-mRFP1-pSEVA331a	pBBR1	The plasmid pSEVA331a harbors the mRFP1 gene positioned downstream of the constitutive promoter J23100, Cm <sup>r</sup>
J23100-mRFP1-pCIMV	pMV01	The plasmid pCIMV harbors the mRFP1 gene positioned downstream of the constitutive promoter J23100, Cm <sup>r</sup>
J23100-mRFP1-pCIPSC	pSC101	The plasmid pCIPSC harbors the mRFP1 gene positioned downstream of the constitutive promoter J23100, Cm <sup>r</sup>
J23100-mRFP1-pC1rep	pC1rep101	The plasmid pC1rep harbors the mRFP1 gene positioned downstream of the constitutive promoter J23100, Cm <sup>r</sup>
J23100-mRFP1-pCIP15a	p15A	The plasmid pCIP15a harbors the mRFP1 gene positioned downstream of the constitutive promoter J23100, Cm <sup>r</sup>
pRedawn-MCS-pSEVA331a	pBBR1	The red light-inducible promoter pRedawn downstream of plasmid pSEVA331a does not express any gene, Cm <sup>r</sup>
pTrc-mRFP1-pSEVA331a	pBBR1	The plasmid pSEVA331a harbors the mRFP1 gene positioned downstream of the IPTG inducible promoter pTrc, Cm <sup>r</sup>
pTrc-B009GT-mRFP1-pSEVA331a	pBBR1	The plasmid pSEVA331a harbors the mRFP1 gene positioned downstream of the IPTG inducible promoter pTrc, RBS is B009GT, Cm <sup>r</sup>
pLux101-mRFP1-pSEVA331a	pBBR1	The plasmid pSEVA331a harbors the mRFP1 gene positioned downstream of the AHL inducible promoter p Lux101, Cm <sup>r</sup>
pln2	pMB1	Empty vector, Cm <sup>r</sup> / Gm <sup>r</sup>
pln2-acsAB1	pMB1	Plasmid for knockdown of <i>acsAB1</i> gene. Cm <sup>r</sup>
pln2-acsAB2	pMB1	Plasmid for knockdown of <i>acsAB2</i> gene. Gm <sup>r</sup>
pln2-acsAB3	pMB1	Plasmid for knockdown of <i>acsAB3</i> gene. Gm <sup>r</sup>
pln2- <i>acsC1</i>	pMB1	Plasmid for knockdown of <i>acsC1</i> gene. Cm <sup>r</sup>
pln2- <i>acsC2</i>	pMB1	Plasmid for knockdown of <i>acsC2</i> gene. Gm <sup>r</sup>
pln2- <i>acsC3</i>	pMB1	Plasmid for knockdown of <i>acsC3</i> gene. Cm <sup>r</sup>
pln2- <i>ccpAx</i>	pMB1	Plasmid for knockdown of <i>ccpAx</i> gene. Cm <sup>r</sup>
pln2- <i>dgc1</i>	pMB1	Plasmid for knockdown of <i>dgc1</i> gene. Gm <sup>r</sup>
pln2- <i>dgc2</i>	pMB1	Plasmid for knockdown of <i>dgc2</i> gene. Cm <sup>r</sup>

Cm<sup>r</sup> and Gm<sup>r</sup> indicate the expression of chloramphenicol and gentamicin resistance genes, respectively.

strains were cultured on Hestrin-Schramm (HS) agar or broth (20 g/L glucose, 5 g/L peptone, 5 g/L yeast, 6.8 g/L disodium phosphate dodecahydrate, and 1.5 g/L citric acid monohydrate) at 30 °C, stationary, or at 180 r/min. Chloramphenicol was used at a concentration of 37 ng/mL for *E. coli* cultivation and 185 ng/mL for *Acetobacteraceae* cultivation. If necessary, cellulase (Sangon Biotech, China) was added at a concentration of 0.4 mg/mL. All the strains were mixed with 70% glycerol at a 1 : 1 volume ratio and then stored in a –80 °C freezer for preservation.

## 2.2 Antibiotic minimum inhibitory concentration (MIC) assay

The bacterial strains were retrieved from the –80 °C freezer and streaked onto HS agar plates, which were then placed in an incubator at 30 °C for 3–4 d. Several colonies were subsequently selected from the agar plates and inoculated into 15 mL centrifuge tubes containing 3–5 mL of HS broth. These tubes were then incubated statically at 30 °C for 2–3 d. Seed cultures were selected on the basis of the presence of cellulose film at the air–liquid interface, the appearance of a clear solution, and the absence of a precipitate at the bottom of the test tubes.

The seed culture was vortexed in a vortex mixer (Scilogex, USA), and 1 mL of the vortexed culture was transferred to fresh HS broth supplemented with cellulase (HS<sup>+</sup>). The culture was then incubated at 30 °C and 180 r/min until it reached the logarithmic growth phase. The culture was subsequently standardized to an optical density at 600 nm

(OD<sub>600</sub>) of 0.5 using fresh HS<sup>+</sup> broth, followed by a 1 : 100 dilution. HS<sup>+</sup> broth, containing twice the concentration of the test antibiotic, was prepared, and 1 mL of each mixture was dispensed into 5 mL centrifuge tubes. One milliliter of previously diluted bacterial culture was added to each centrifuge tube containing varying concentrations of the antibiotic and thoroughly mixed. All the tubes were then incubated at 30 °C, and the growth of each culture was visually inspected and recorded for 6 d. The lowest antibiotic concentration without visible bacterial growth was determined as the minimum inhibitory concentration (MIC) for the respective test strain.

## 2.3 Growth curve measurement

The seed broth was cultured following a previously described method. The seed broths of the three tested strains were vortexed, inoculated into 50 mL of fresh HS<sup>+</sup> broth, and then incubated until they reached the logarithmic growth stage at 30 °C and 180 r/min. After centrifugation at 4100 r/min for 12 min, the bacterial pellet was resuspended in fresh HS<sup>+</sup> broth. The OD<sub>600</sub> values of the three resuspended cultures were standardized to a uniform value of 0.5. Subsequently, a 1 : 10 dilution of the resuspended cultures with a final volume of 100 mL was prepared in 250 mL conical flasks. The test strains were cultured in a shaker at 30 °C and 180 r/min to measure bacterial growth curves during shaking. The OD<sub>600</sub> values of the test strains were measured every 2 h via a UV spectrophotometer (Biochrom, Ultrospec 10 Cell Density Meter, UK). For static bacterial growth curve measurements, the diluted bacterial mixture was permitted to stand in 14 mL

centrifuge tubes. Subsequently, 150  $\mu\text{L}$  of the bacterial mixture was aspirated into a 96-well plate at approximately 5-h intervals, and the  $\text{OD}_{600}$  values of the bacteria were measured via a microplate reader (Synergy H1, BioTek, USA).

#### 2.4 Bacterial cellulose film yield analysis

The cellulose culture procedure was established on the basis of the protocol of Liu et al.<sup>[23]</sup>. The seed broths of the three tested strains were vortexed, inoculated into 30 mL of fresh  $\text{HS}^+$  broth, and then incubated until they reached the logarithmic growth stage at 30 °C and 180 r/min. Following centrifugation at 4100 r/min for 12 min, the bacterial pellet was washed twice with sterile 0.9% NaCl. The bacteria were subsequently resuspended in fresh  $\text{HS}^+$  broth and diluted 1 : 25 after their  $\text{OD}_{600}$  values were standardized to 0.5. Notably, to characterize the effects of different concentrations of the inducers isopropyl  $\beta$ -D-1-thiogalactopyranoside (IPTG) or N-acyl homoserine lactone (AHL) on BC productivity, the corresponding concentration of the inducer (IPTG or AHL) should be added to the dilution solution. Finally, the diluted bacterial mixture was dispensed at 3 mL per well into a 12-well plate at 30 °C.

The treatment of BC films followed the protocol of Mangayil et al.<sup>[28]</sup>. After incubation for 4 d, the BC films were collected in 50 mL centrifuge tubes. These films were washed (optionally heated in a microwave) twice with ultrapure water (Milli-Q, EMD Millipore, Germany) and then immersed in 0.1 M NaOH solution at 65 °C until they turned completely white. Following several washes with ultrapure water, the BC films were incubated in ultrapure water at 65 °C overnight to enhance impurity removal. Finally, the BC films were placed in clean dishes and dried at 65 °C for 24 h. The dry weights of the BC films were measured via an analytical balance (Sartorius, Germany).

#### 2.5 Plasmid transformation efficiency and frequency analysis

The plasmid transformation protocol was established on the basis of the protocol of Mangayil et al.<sup>[28]</sup>. Briefly, the pre-prepared seed stock of the test strain was inoculated into 50 mL of fresh  $\text{HS}^+$  broth and incubated at 30 °C and 180 r/min until the logarithmic phase was reached, followed by centrifugation at 4100 r/min for 12 min. The centrifuged cells were then washed twice with 10 mL of sterile, ice-cold 1 mM 4-(2-hydroxyethyl)-1-piperazineethanesulfonic acid (HEPES, pH = 7.0) and subsequently with 10 mL of sterile, ice-cold 15% glycerol. The bacterial mixture was resuspended in 15% glycerol, and the  $\text{OD}_{600}$  value was standardized to 19.8.

For the transformation process, 600–900 ng of plasmid was added to every 95  $\mu\text{L}$  of the prepared electrocompetent cells, mixed thoroughly, and then transferred to 2 mm electroporation cuvettes (Bio-Rad, USA). Electroporation was performed at 2.5 kV (Bio-Rad, USA). The pulsed cells were immediately resuspended in 1 mL of prewarmed  $\text{HS}^+$  broth, transferred to 15 mL tubes, and then incubated at 30 °C and 180 r/min for 16 h. The bacteria were collected at 4100 r/min for 12 min, the bacterial precipitate was resuspended in 200  $\mu\text{L}$  of sterile 0.9% NaCl, and the resuspension solution was diluted in a gradient with 0.9% NaCl ( $10^1$ ,  $10^2$ ,  $10^3$ ,  $10^4$ ,  $10^5$  and  $10^6$ ). Subsequently, 100  $\mu\text{L}$  of bacterial mixture from undiluted,  $10^1$ - and  $10^2$ -fold dilutions was spread on HS agar

plates containing chloramphenicol. One hundred microlitres of bacterial mixture from  $10^3$ -,  $10^4$ -,  $10^5$ - and  $10^6$ -fold dilutions were spread on HS agar plates. The number of single clones in the plates was counted after all the plates were incubated in a 30 °C incubator for 4–7 d. The calculation methods for plasmid transformation efficiency and frequency are consistent with those described in Ref. [29].

#### 2.6 Inducible promoter characterization

All test strains were cultured in  $\text{HS}^+$  broth containing chloramphenicol and cellulose ( $\text{HS}^{++}$ ) at 30 °C and 180 r/min until they reached the stationary phase. The strains were subsequently diluted 1 : 200 in fresh  $\text{HS}^{++}$  broth and incubated overnight until they reached the logarithmic growth phase. The bacterial mixture was then centrifuged at 4100 r/min for 12 min, and the pellet was subsequently resuspended in fresh  $\text{HS}^{++}$  broth. The  $\text{OD}_{600}$  values of the resuspended strains were adjusted to 0.2, and the strains were mixed with the pre-prepared inducer-containing  $\text{HS}^{++}$  broth at a 1 : 1 volume ratio. After thorough mixing, 150  $\mu\text{L}$  of each sample was dispensed into a black 96-well plate in triplicate. The 96-well plate was incubated at 30 °C in a microplate reader (SpectraMax iD5, USA). The  $\text{OD}_{600}$  and fluorescence values (590–630 nm) were measured every 2 h.

#### 2.7 Gene knockout experiment

Several recombinant plasmids containing homologous fragments of the target genes were constructed and validated through sequencing. Following validation, the confirmed plasmids were introduced into the *G. hansenii* ATCC 53582 strain via electroporation as previously described. After overnight incubation, the bacterial mixture was spread evenly onto HS agar supplemented with either chloramphenicol or gentamicin and left to grow for 3–5 d. Single colonies were then selected and streaked onto new HS agar plates containing the corresponding antibiotics for further incubation. If the initial single colonies are relatively large, the streaking step can be omitted.

The cells from the streaked plate were subsequently suspended in 30  $\mu\text{L}$  of sterile water, followed by heat treatment at 95 °C for 15 min and centrifugation at 1300 r/min for 2 min. The resulting supernatant, containing the DNA template, was utilized for PCR identification. Positive strains harboring the correct fragment were identified, and the corresponding fragments were excised from the gel and sent for sequencing to confirm their authenticity.

## 3 Results

### 3.1 The *G. hansenii* ATCC 53582 strain has the highest cellulose film production capacity

As previously mentioned, BC production is an important characteristic of *Acetobacteraceae* strains. Therefore, the cellulose film production capacity of strains *G. hansenii* ATCC 53582, *K. rhaeticus* iGEM, and *G. xylinus* 700178 was initially analyzed. Specifically, the BC films produced by these strains were analyzed after they were cultured in 50 mL centrifuge tubes and 12-well plates for 4 d. The results revealed significant differences in cellulose film production

capacity among the three strains (Fig. 1a and b). The BC film produced by the *G. hansenii* ATCC 53582 strain was the thickest, followed by that produced by *K. rhaeticus* iGEM (Fig. 1a). The dry weight of the BC films produced by *G. hansenii* ATCC 53582 in the 12-well plate exceeded that of *K. rhaeticus* iGEM and *G. xylinus* 700178 by 3.64 and 6.94 times, respectively (Fig. 1b).

The growth curves of the three bacteria were subsequently monitored under both stationary (Fig. 1d) and shaking conditions (Fig. 1e) to reveal any disparities in their growth characteristics or biological behaviors. The results indicate that under stationary cultivation, the proliferation of these three strains was extremely slow (Fig. 1c, d). The fastest proliferating strain, *G. hansenii* ATCC 53582, had a division time of 13.16 h, which was 0.57 and 0.69 times greater than those of *K. rhaeticus* iGEM and *G. xylinus* 700178, respectively (Fig. 1c). Interestingly, there was no significant difference in the division times among the three strains during the shaking state, with average cell division times ranging from 2.65 to 2.69 h (Fig. 1f).

Taken together, the *G. hansenii* ATCC 53582 strain

presented the highest cellulose film production and proliferation ability among the three strains during stationary incubation.

### 3.2 *K. rhaeticus* iGEM demonstrates advanced plasmid transformation efficiency and replication stability

Antibiotics play a vital role in both screening and maintaining the stability of exogenous plasmids within engineered bacteria<sup>[30]</sup>. Therefore, the initial step involved testing the sensitivity of the three *Acetobacteraceae* strains to seven commonly utilized antibiotics. The results revealed that the *G. hansenii* ATCC 53582 strain displayed relatively lower sensitivity to the tested antibiotics than the *G. xylinus* 700178 and *K. rhaeticus* iGEM strains did (Fig. 2a). In particular, the *G. hansenii* ATCC 53582 strain was resistant to aminoglycoside antibiotics (gentamicin and kanamycin), whereas the *G. xylinus* 700178 and *K. rhaeticus* iGEM strains were susceptible (Fig. 2a).

Plasmid transformation is a widely utilized technique in genetic engineering research. To assess the difficulty of genetic engineering operations on the three strains, the efficiency and

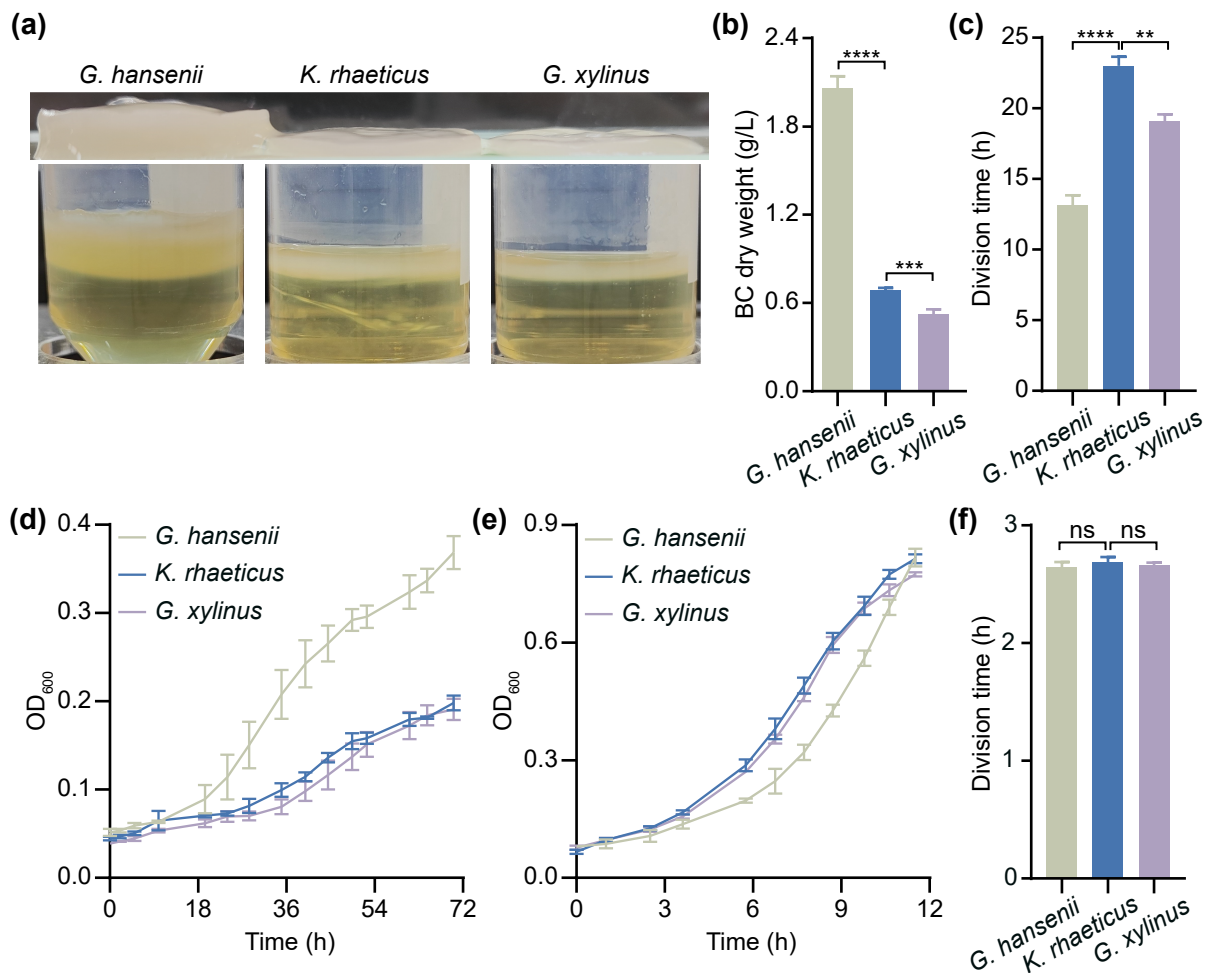


**Fig. 1.** Analysis of basic information of three *Acetobacteraceae* strains. (a) Photograph of the cellulose films produced by the three test strains after 4 d of incubation in 50 mL centrifuge tubes. (b) Dry weights of the cellulose films formed by the three test strains after 4 d of incubation in 12-well plates. The division times (c) and growth curves (d) of the three test strains during static incubation. The growth curves (e) and division times (f) of the three test strains during shaking incubation. The error bars represent the means  $\pm$  SDs;  $n = 3, 4$ ; ns = not significant; \*\*  $P \leq 0.01$ ; \*\*\*  $P \leq 0.001$ ; \*\*\*\*  $P \leq 0.0001$  (Student's  $t$  test).

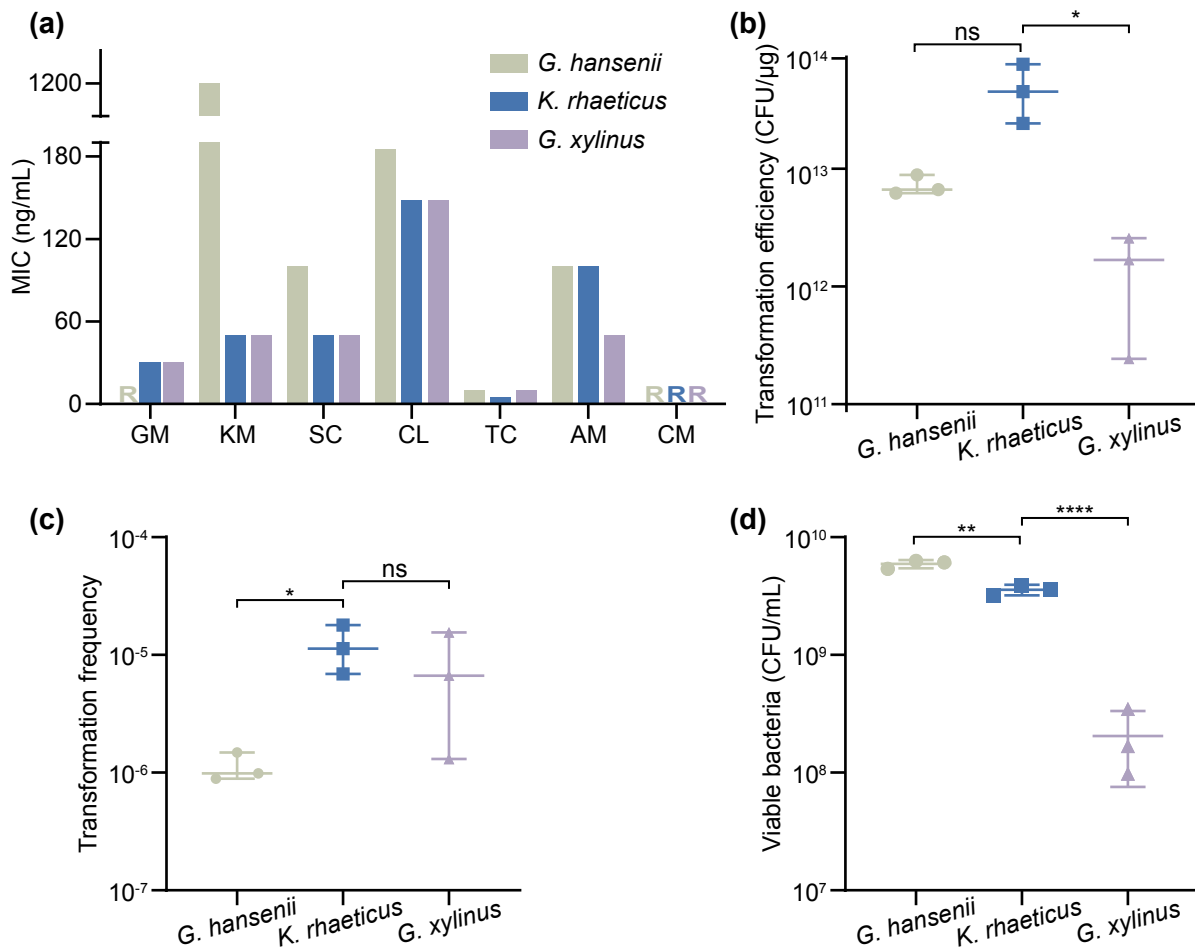


**Fig. 2.** Plasmid features analysis. (a) Minimum inhibitory concentrations (MICs) of seven antibiotics against the three test strains. R indicates that the test strains can grow in HS broth containing 1200 ng/mL antibiotics; GM, KM, SC, CL, TC, AM, and CM represent gentamicin, kanamycin, spectinomycin, chloramphenicol, tetracycline, ampicillin, and carbenicillin, respectively. Plasmid transformation efficiency (b) and frequency (c) of the three test strains. (d) Enumeration of surviving three test strains on HS agar plates after electroporation. The error bars represent the means  $\pm$  SDs;  $n = 3$ ; ns = not significant; \* $P \leq 0.05$ ; \*\* $P \leq 0.01$ ; \*\*\*\* $P \leq 0.0001$  (Student's  $t$  test).

frequency of plasmid (J23100-mRFP1-pSEVA331a) transformation for each strain were evaluated. By quantifying single clones on HS agar plates with and without resistance postelectroporation, higher plasmid transformation efficiencies were observed for the *K. rhaeticus* iGEM and *G. hansenii* ATCC 53582 strains, with increases of 32.76-fold and 4.83-fold, respectively, in contrast to those of the *G. xylinus* 700178 strain (Fig. 2b). However, the plasmid transformation frequency was greater in the *G. xylinus* 700178 strain than in the *G. hansenii* ATCC 53582 strain (Fig. 2c). This variation can be attributed to the significantly lower count of surviving bacteria of the *G. xylinus* 700178 strain on the HS agar plates without antibiotics than on the other two strains (Fig. 2d).

Testing the ori is an important indicator for evaluating the ability of a plasmid to replicate within bacteria. Five different ori sequences were inserted into the plasmid and then transformed into the three strains to conduct replication experiments. After PCR identification and DNA sequencing, the results revealed that all five plasmids (pBBR1, pMV01, pSC101, pCrep101, and p15a) could replicate in the *G. hansenii* ATCC 53582 strain, whereas three plasmids

(pBBR1, pMV01, and pCrep101) demonstrated replication capability in the *G. xylinus* 700178 strain, and only two plasmids (pBBR1 and pMV01) could replicate in the *K. rhaeticus* iGEM strain (Fig. 3a). Notably, ori pCrep101 underwent deletion mutations after being transformed into the *G. hansenii* ATCC 53582 and *G. xylinus* 700178 strains, and their new sequences are listed in Table 3.

The stability of plasmids directly impacts their outcomes and application efficacy in gene expression and genetic engineering research. However, experiments have shown that only J23100-mRFP1-pSEVA331a (pBBR1) could be stably maintained within the three strains containing different plasmids after three months of incubation (Fig. 3b, c). Additionally, J23100-mRFP1-pCIMV (pMV01) was stable within the *K. rhaeticus* iGEM strain, whereas the remaining plasmids were lost during this period (Fig. 3b, c).

### 3.3 IPTG-inducible promoter pTrc shows a low dynamic range in *Acetobacteraceae*

Inducible promoters are crucial for achieving precise regulation of gene expression in bacteria<sup>[31]</sup>. The pTrc promoter is a well-known and widely used inducible promoter in

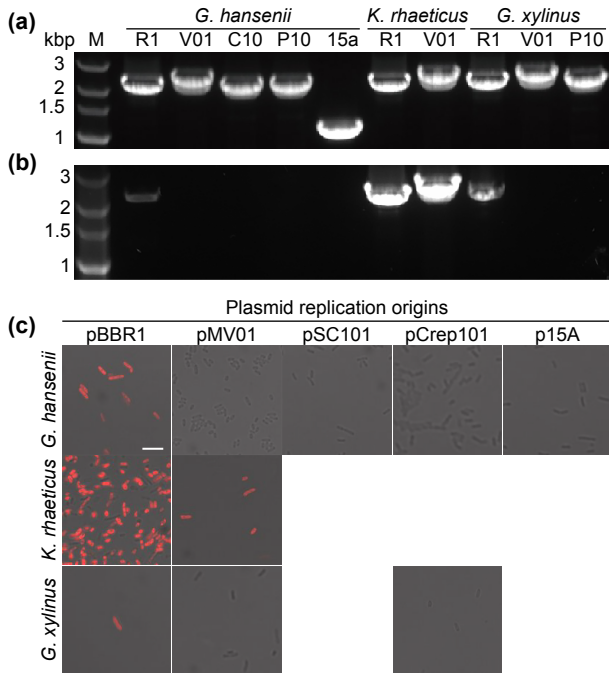


**Fig. 3.** Plasmid replication and stability analysis. Electropherograms of replicable (a) and stabilizable (b) origins of plasmid replication within the three test strains. M refers to the DNA marker, and R1, V01, C01, P10, and 15a represent the plasmid replication origins pBBR1, pMV01, pSC101, pCrep101, and p15a, respectively. (c) Merged image of the strains in panel a after three months of static culture at room temperature; scale bar, 5  $\mu$ m.

**Table 3.** The sequence of the plasmid origin of replication pCrep101 used in this study.

Ori	Sequence
pCrep101	tcagatcctccgtatttagcagatgftctctagtggtgctgtgttttgcgtgagc catgagaacgaaccattgatgacatacttctgcatgcaactcaaaaattttgcctc aaaactggtgagctgaattttgacgttaaagcagctgtagtgttttcttagtccgtt aTgtagtgaggaaatctgatgaatggtggtgattttgcaccattcattttatctg gttgttctcaagttcggtagacagatcattgtctatctagttcaactggaaaatcaa cgtatcagtcggcgccctgcctatcaaccaccaatttcattgctgtaagtgtta aatcttactattggttcaaaaccattggtgaagcctttaaactcatggtgatttt tcaagcattaaactgaactaaatcatcaaggctaatctctatatttgccttgtagttt tcttttggtagttcttttaataaccactcaaaactcctcatagagattggtttcaaaag acttaacatgtccagattatatttgaatttttaactggaagataaggcaaat ctcttcaactaaaactaattctaatcttgcctgagaactggcatagtttgcactg gaaaatcacaagccttaaccaaggattcctgattccacagttctgctcatcagc tctctggtgcttttagcctaatacaccataaagcatttccctactgatgtcatcatcga Acgtattggtataatgaacgataaccgctccttcttctgtagggtttcaatcgt ggggtgagtagtgcacacagcataaaattagctgggttcctgctccggttaagtc atagcgactaatcgtagtcttctgtgaaaacaactaactcagacatacctca attgctgtagtgatttatacactataccaattgagatgggctagtcgatgataatta ctagtccttttcttctgagttggtgatctgtaattctgctagaccttctggtgaaa ctgtaaatctgctgaccctctgtaaatccgctagaccttctggtttttttttat attcaagtgttataattatagataaaagaaagataaaaaagataaaaaagaata gatccagccctgtgtataactcactacttttagtcagttccgcagattacaagaagga tctgcacaacgctgttctcctctcaaaaacagaccttaaaaccctaaaggcctaa gtgaccctcgcaagctgggcaaatcgtaatttcttctgctccgaccatc aggcaactgagtcgctgttcttctgacattcagttcgtcgcctcagggctcctg cagtgaaatgggggtaaatgcaactacagcgccctttatgattcatcaaggaaa ctaccataatacaagaaaagcccgtcacggcctctcaggggcgtttatggcgg gtctgctatggtgctactctgacttttctgtctcagcagttcctgacctgatttcc agtctgaccactcggattatcccgtgacaggtcattcagactgctaatgacacca gtaaggcagcggatcatcaac

molecular biology research. The inducible expression of the pTrc promoter in the *G. hansenii* ATCC 53582, *K. rhaeticus* iGEM, and *G. xylinus* 700178 strains was comprehensively characterized via the use of the fluorescent protein mRFP1 as a reporter (Fig. 4a). By replacing the ribosome binding site (RBS) of the protein mRFP1 with two RBSs of varying strengths, six engineered strains (containing the plasmids pTrc-mRFP1-pSEVA331a or pTrc-B009GT-mRFP1-pSEVA331a) were subsequently constructed (Fig. 4a). The RBS sequence was derived from previous research<sup>[32]</sup>. To facilitate differentiation, the mutations obtained at the 9th position of RBS B0034 in the literature<sup>[32]</sup> were named B009GT. The nomenclature of these strains was derived from a combination of the host strain and the name of the mRFP1 upstream RBS. Consequently, the engineered strains were named H-trc, H-9trc, R-trc, R-9trc, X-trc, and X-9trc, respectively (Fig. 4a). The relative fluorescence values (RFP/OD<sub>600</sub>) of the six strains were analyzed after 12 h of cultivation with various concentrations of the inducer IPTG. For all the test strains, except for the H-trc strain, the relative fluorescence values increased as the concentration of the inducer increased (Fig. 4b–d). Specifically, the H-trc and H-9trc strains engineered with the *G. hansenii* ATCC 53582 strain as the host exhibited 4.89- and 6.39-fold increases in relative fluorescence values following induction with IPTG at a concentration of 1.0 mM compared with the uninduced levels (IPTG concentration of 0 mM) (Fig. 4b). Among the two engineered strains based on the *K. rhaeticus* iGEM strain, only the R-9trc strain presented a 2.15-fold increase in relative fluorescence values following induction compared with the uninduced strains (Fig. 4c). The background fluorescence of the R-trc strain was significantly greater, approximately 132.23 times greater than that of the R-9trc strain (Fig. 4c). Therefore, the absence of an IPTG response in the R-trc strain is likely due to excessive background expression. In the engineered strains X-trc and X-9trc, when the *G. xylinus* 700178 strain was used as the host, the fold changes in relative fluorescence values following induction were 1.98 and 2.17, respectively (Fig. 4d). Compared with the X-9trc strain, the X-trc strain presented stronger background fluorescence values, with a 1.49-fold increase (Fig. 4d). In summary, the expression of the promoter pTrc in different host strains is influenced by the strength of the upstream RBS of the target protein.

The induction curves of the six strains in HS<sup>++</sup> broth containing 1.0 mM IPTG were subsequently examined. The results revealed an increase in the relative fluorescence values of the six strains over time. Compared with those at time point 0, the fluorescence values of H-trc, H-9trc, R-trc, R-9trc, X-trc, and X-9trc increased by 3.84, 2.68, 1.63, 2.14, 4.21, and 7.62 times, respectively, after 12 h of induction (Fig. 4e–g).

To further evaluate the optimal IPTG concentration, the effects of various IPTG concentrations on the growth of the six engineered strains and their correction strains (strains without the pTrc and mRFP1 fluorescent protein promoters) were examined. The results indicated that the tested IPTG concentrations had no significant effect on bacterial growth (Fig. 4h) (data not shown). Importantly, the tested IPTG concentrations did not affect the cellulose production capacity of the host strains (Fig. 4i).

In summary, the pTrc promoter can be effectively induced in *G. hansenii* ATCC 53582, *K. rhaeticus* iGEM, and



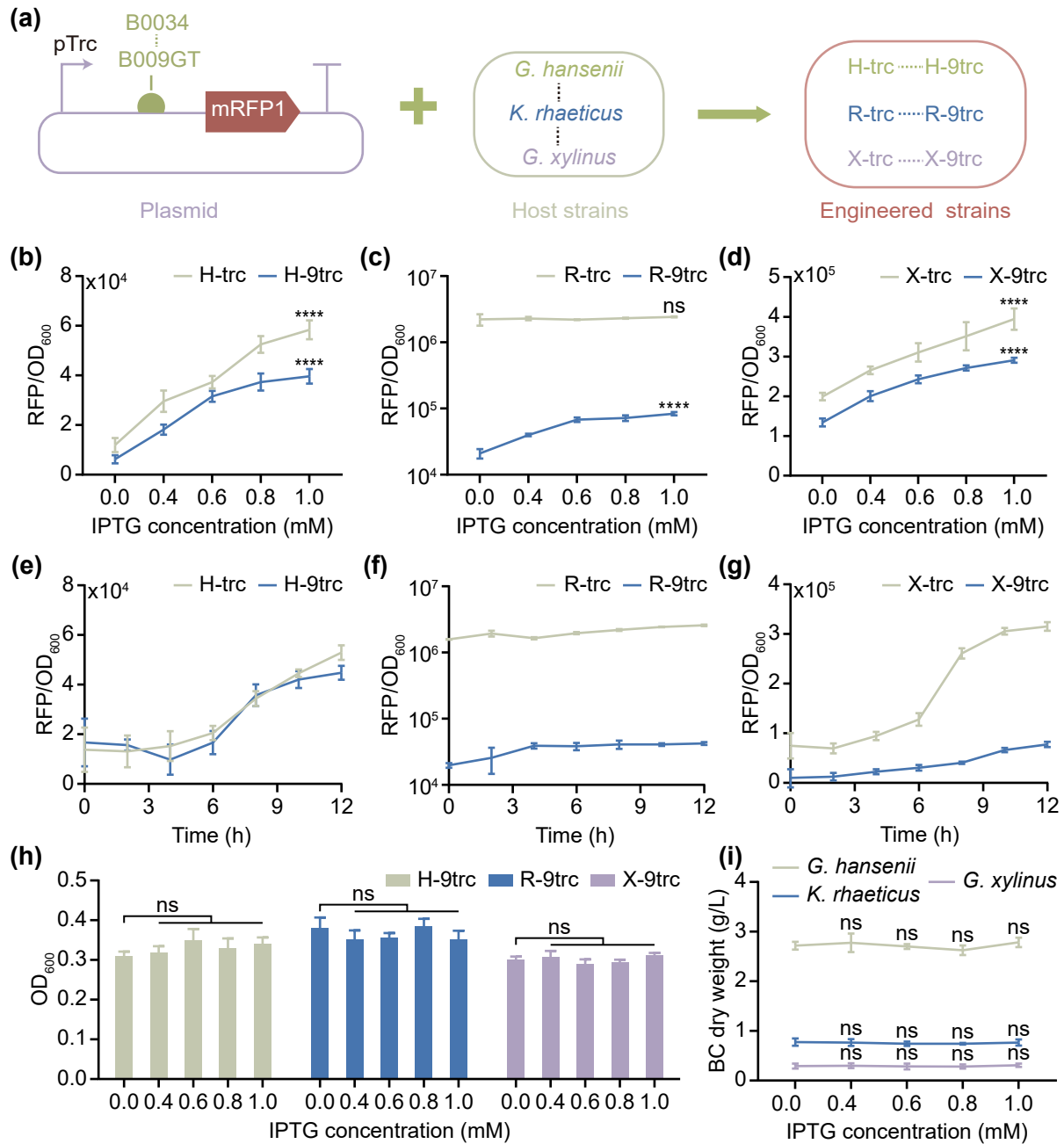


**Fig. 4.** Characterization of the promoter pTrc. (a) Schematic diagram of the engineered strains carrying the pTrc promoter that was tested. Dose response of the inducible promoter pTrc in *G. hanseni* ATCC 53582 (b), *K. rhaeticus* iGEM (c) and *G. xylinus* 700178 (d) to varying IPTG concentrations and RBS intensities after 12 h of induction. (e) Induction curves of the H-trc and H-9trc strains at a 1.0 mM IPTG concentration. (f) Induction curves of the R-trc and R-9trc strains at a 1.0 mM IPTG concentration. (g) Induction curves of the X-trc and X-9trc strains at a 1.0 mM IPTG concentration. (h) OD<sub>600</sub> values of strains H-9trc, R-9trc and X-9trc after incubation in HS<sup>+</sup> containing different IPTG concentrations for 12 h. (i) The dry weights of BC films from *G. hanseni* ATCC 53582, *K. rhaeticus* iGEM, and *G. xylinus* 700178 incubated in HS<sup>+</sup> broth with varying IPTG concentrations. The error bars represent the means ± SDs; n = 3, 4, significant differences among the control group (IPTG concentration of 0 mM) and the other groups were computed via one-way ANOVA; ns = not significant; \*\*\*\* P ≤ 0.0001.

*G. xylinus* 700178 strains. The expression of the target protein can be adjusted by modifying the strength of the RBS upstream of the target gene to modulate the background expression and dynamic range of the protein.

### 3.4 The AHL-inducible promoter pLux101 is highly dynamic in *Acetobacteraceae*

Low-background, high-induction promoters are pivotal for

achieving precise control of gene expression, increasing protein production yield, and providing researchers with greater control over experimental systems. Research conducted by Florea et al.<sup>[23]</sup> on the *K. rhaeticus* iGEM strain demonstrated the superiority of the pLux101 promoter, which is induced by AHL, in terms of lower background expression and a higher induction rate than the anhydrotetracycline (ATc)-induced promoter. Hence, to comprehensively characterize the

pLux101 promoter within the *G. hansenii* ATCC 53582, *K. rhaeticus* iGEM, and *G. xylinus* 700178 strains, plasmids carrying the pLux101-regulated fluorescent protein mRFP1 were introduced into each of the three strains. The engineered strains were denoted H-plux, R-plux, and X-plux, respectively. After 12 h of cultivation in HS<sup>+</sup> broth with various AHL concentrations, the fluorescence intensities of the H-plux, R-plux, and X-plux strains were measured. The results demonstrated their high sensitivity to AHL, with a significant increase in fluorescence intensity with increasing concentrations of AHL (Fig. 5a). Compared with that of the uninduced control group, the fluorescence intensity of the H-plux, R-plux, and X-plux strains increased by 16.53-, 32.39-, and 7.29-fold, respectively, at an AHL concentration of 10 nM (Fig. 5a). Furthermore, at an AHL concentration of 500 nM, the fold change in fluorescence intensity among the three strains reached 176.86, 216.71, and 87.28, respectively (Fig. 5a). Subsequently, the induction curves of the three test strains at an AHL concentration of 500 nM were analyzed, revealing their rapid response to AHL, reaching saturation within approximately 6 h after induction (Fig. 5b). Following 2 h of induction, the fluorescence intensities of the H-plux, R-plux, and X-plux strains were 24.31-, 26.92-, and 6.52-fold greater, respectively, than those at the initial time point (0) (Fig. 5b). Moreover, following 12 h of induction, the fold changes in fluorescence intensity for the H-plux, R-plux, and X-plux strains were 198.89, 385.87, and 37.19, respectively (Fig. 5b).

The impacts of different AHL inducer concentrations on the growth of the test strains were subsequently assessed. The results showed that the growth of the H-plux and R-plux strains was influenced by the AHL concentration, whereas their corresponding correction strains remained unaffected (Fig. 5d–f). This observation led to the inference that the inhibitory effect of high concentrations of AHL on the growth of H-plux and R-plux strains might be attributed to an excessively high activation rate of the promoter within those strains. Furthermore, the effects of different AHL concentrations on cellulose production in the *G. hansenii* ATCC 53582, *G. xylinus* 700178, and *K. rhaeticus* iGEM strains were compared. The results indicated that the AHL concentrations used in the experiment did not significantly impact the cellulose film production ability of these host strains (Fig. 5c).

In conclusion, the pLux101 promoter presented a relatively high induction rate among the *G. hansenii* ATCC 53582, *K. rhaeticus* iGEM, and *G. xylinus* 700178 strains. Additionally, the AHL inducer used in the experiment had no discernible effect on the growth or BC film production capability of the tested strains.

### 3.5 Essential genes for cellulose production in the *G. hansenii* ATCC 53582 strain

The synthesis of BC films within *Acetobacteraceae* is a complex, precise, and highly regulated process<sup>[27]</sup> that predominantly relies on the *Acetobacter* cellulose synthase (*acs*) operon, cellulose complementing factor (*ccpAx*), and the second messenger cyclic diguanylate (c-di-GMP)<sup>[33]</sup>. The *acs* operon typically contains three essential genes, *acsA*, *acsB*, and *acsC*, and one nonessential gene, *acsD*. Additionally, in some bacteria, the proteins AcsA and AcsB are expressed by the

*acsAB* gene. Within the genome of the *G. hansenii* ATCC 53582 strain, three genes are homologous to the cellulose synthases *acsAB* and *acsC*, whereas two genes are homologous to the c-di-GMP synthase *dgc*<sup>[34]</sup>. Given that not all of these homologous genes are necessarily involved in BC synthesis<sup>[33]</sup>, an analysis of nine potential genes within the genome of the *G. hansenii* ATCC 53582 strain was conducted to ascertain which genes are indeed essential for cellulose synthesis<sup>[33–35]</sup> (Table 4). Specifically, the *pln2* single recombination technique was applied to knock out these genes from the genome of the *G. hansenii* ATCC 53582 strain (Fig. 6a)<sup>[36]</sup>. Nine variant strains were subsequently generated (Fig. 6b), named  $\Delta$ AB1,  $\Delta$ AB2,  $\Delta$ AB3,  $\Delta$ C1,  $\Delta$ C2,  $\Delta$ C3,  $\Delta$ ccp,  $\Delta$ dgc1, and  $\Delta$ dgc2, on the basis of the knockout genes. Notably, two homologous segments are present in the genomes of variant strains obtained via single recombination techniques (Fig. 6a, indicated by A in the red box), resulting in the appearance of two bands in the electropherogram obtained via PCR identification (Fig. 6b).

The analysis of the variant strains revealed that four variant strains,  $\Delta$ AB1,  $\Delta$ C1,  $\Delta$ ccp, and  $\Delta$ dgc2, lost the ability to generate BC films (Fig. 6c). Ultimately, by employing plasmids to restore the expression of the relevant genes, the ability to produce cellulose film was successfully restored in all four strains (Fig. 6d).

In conclusion, the genes *acsAB1*, *acsC1*, *ccpAx*, and *dgc2* are crucial for BC film production in the *G. hansenii* ATCC 53582 strain.

## 4 Discussion

The genetic background and growth environment of the chassis strain are important factors that influence the natural environment and the synthesis of specific products adapted by engineered strains<sup>[5,6]</sup>. Therefore, there is an increasing focus among researchers on the development and study of nonmodel strains<sup>[9,37]</sup>. As previously mentioned, *Acetobacteraceae* holds immense value in various applications<sup>[11,38,39]</sup>. Establishing synthetic biology kits for *Acetobacteraceae* can significantly accelerate the investigation of its genetic background by researchers and facilitate its utilization as a key tool for the sustainable production of biocompatible materials and pharmaceuticals. In this study, precise guidance for selecting suitable host strains was offered by comparing the fundamental characteristics of three prevalent BC-producing strains. The experimental results suggest that *G. hansenii* ATCC 53582 and *K. rhaeticus* iGEM are considered the optimal host strains for regulating bacterial cellulose film production, as they exhibit superior performance in terms of cellulose film production (Fig. 1a and b), plasmid transformation efficiency (Fig. 2b), and plasmid stability (Fig. 3b, c). Thus, a concentrated effort to advance the establishment of synthetic biology element libraries within the *G. hansenii* ATCC 53582 and *K. rhaeticus* iGEM strains is advocated for in subsequent investigations.

Inducible promoters are crucial tools for researchers to manipulate gene expression precisely in bacteria to control desired products or functions<sup>[37]</sup>. Hence, in this work, the induction curves of two inducible promoters, pLux101 and pT<sub>rc</sub>,

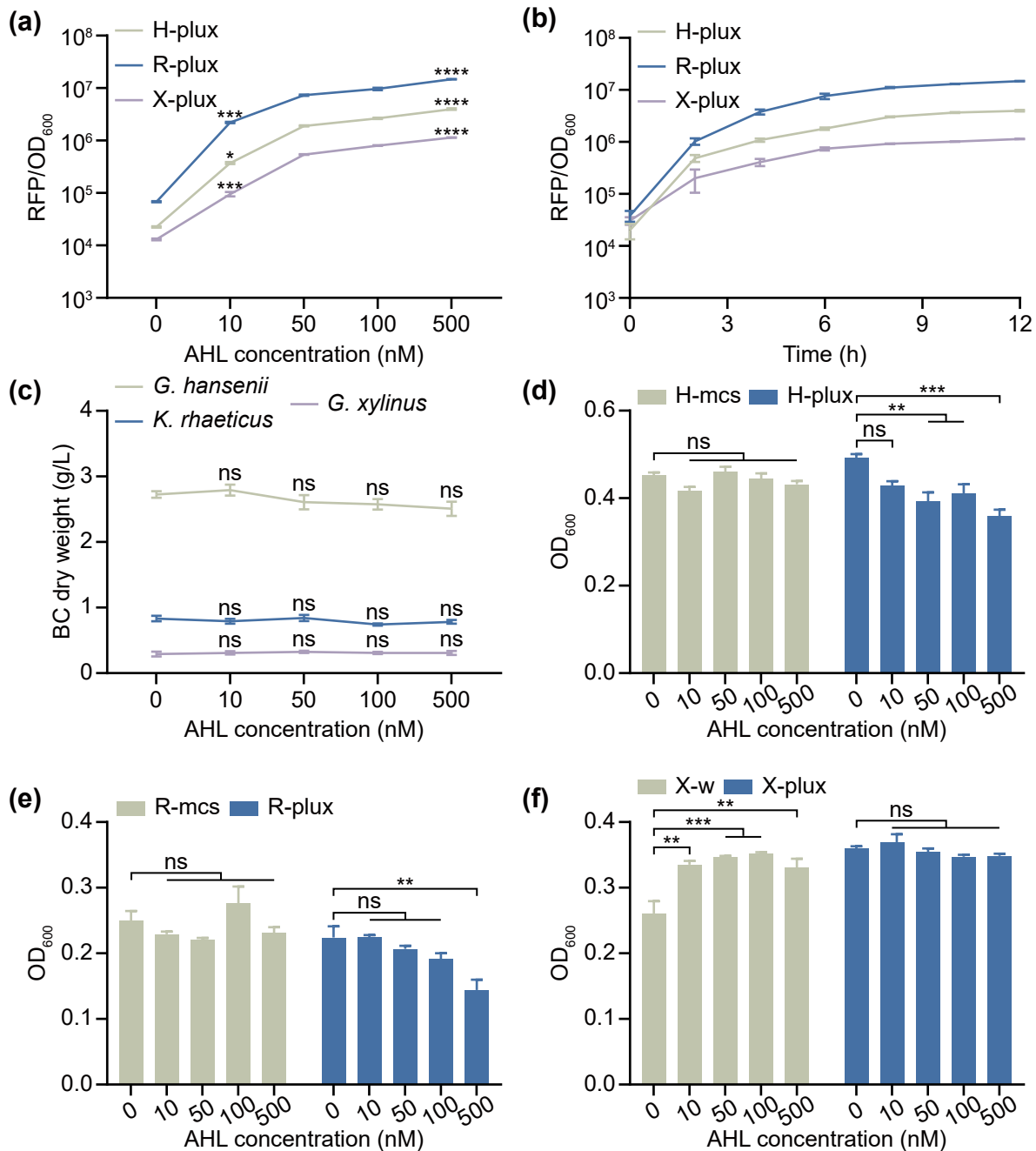


**Fig. 5.** Characterization of the promoter pLux101. (a) Dose response of the H-plux, R-plux, and X-plux strains to different concentrations of AHL after 12 h of induction. (b) Induction curves of the H-plux, R-plux, and X-plux strains at a concentration of 500 nM AHL. (c) BC dry weight films from the *G. hansenii* ATCC 53582, *K. rhaeticus* iGEM, and *G. xylinus* 700178 strains after incubation in HS<sup>+</sup> broth with varying AHL concentrations for 4 d. (d) OD<sub>600</sub> values of H-plux and its correction strains (H-mcs) incubated with various AHL concentrations for 12 h. (e) OD<sub>600</sub> values of R-plux and its correction strains (R-mcs) incubated with various AHL concentrations for 12 h. (f) OD<sub>600</sub> values of X-plux and its correction strains (wild-type *G. xylinus* 700178 strain, X-w) incubated with varying AHL concentrations for 12 h. The error bars represent the means  $\pm$  SEMs;  $n = 3, 4$ , significant differences among the control group (AHL concentration of 0 nM) and the other groups were computed via one-way ANOVA; ns = not significant; \*  $P \leq 0.05$ , \*\*  $P \leq 0.01$ , \*\*\*  $P \leq 0.001$  and \*\*\*\*  $P \leq 0.0001$ .

were characterized in the three strains. This study revealed that the promoter pTrc can be induced in all three strains, albeit with a relatively low induction rate (Fig. 4a–c). Conversely, the pLux101 promoter has a relatively high dynamic range, with fluorescence values ranging from 87.28 to 216.71 across the three strains (Fig. 5a). However, excessive activation of the pLux101 promoter can harm the growth of

engineered strains (Fig. 5d–f). Thus, careful selection of the induction promoter and control of the inducer concentration during experiments are crucial for achieving precise manipulation of gene expression in bacteria and mitigating potential negative impacts on growth and other cellular processes. Importantly, the strength of the RBS upstream of the target protein is a critical factor influencing the background expression

**Table 4.** Genes associated with bacterial cellulose production in the genome of the *G. hansenii* ATCC 53582 strain.

Gene	Describe	Protein ID
<i>acsAB1</i>	Cellulose synthase <i>acsAB</i> homologous sequence	CUW46506.1
<i>acsAB2</i>	Cellulose synthase <i>acsAB</i> homologous sequence	CUW48393.1
<i>acsAB3</i>	Cellulose synthase <i>acsAB</i> homologous sequence	CUW47136.1
<i>acsC1</i>	Cellulose synthase <i>acsC</i> homologous sequence	CUW46507.1
<i>acsC2</i>	Cellulose synthase <i>acsC</i> homologous sequence	CUW48390.1
<i>acsC3</i>	Cellulose synthase <i>acsC</i> homologous sequence	CUW47137.1
<i>ccpAX</i>	Cellulose-complementing	CUW46505.1
<i>dgc1</i>	Diguanylate cyclase <i>dgc</i> homologous sequence	CUW46098.1
<i>dgc2</i>	Diguanylate cyclase <i>dgc</i> homologous sequence	CUW48224.1

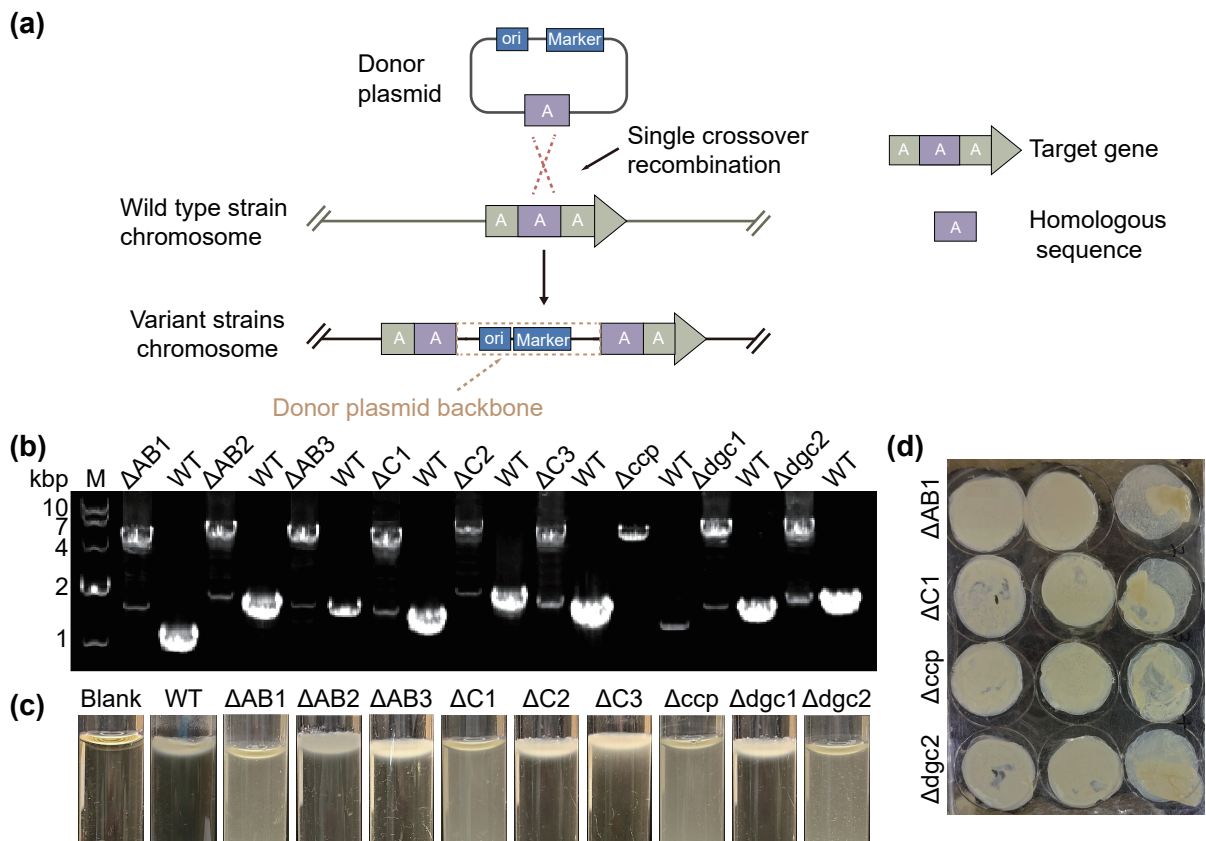


**Fig. 6.** Screening of critical genes for bacterial cellulose production. (a) Schematic diagram of pln2 single recombination technology. (b) PCR identification of the nine variant strains obtained via single recombination methods. (c) BC film production of the wild-type *G. hansenii* ATCC 53582 strain (WT) and nine variant strains after stationary incubation in HS broth. (d) BC film production in 12-well plates of four variant strains after complementation of the corresponding genes.

and dynamic range of the induction promoter (Fig. 4d–f). Adjusting the strengths of pre-RBS can significantly increase the precision of regulating the expression of the target protein. In conclusion, the characterization of these two inducible promoters provides theoretical guidance for regulating gene expression within these strains. However, the two promoters characterized rely on specific chemical inducers for activation, which lack sufficient spatiotemporal resolution and are not easily removed after their addition. Therefore, future research should investigate the use of physical inducers with higher spatiotemporal resolution<sup>[40,41]</sup>, especially light-inducible promoters<sup>[42–46]</sup>, to achieve more precise control and regu-

lation of gene expression. This, in turn, could create new opportunities for manipulating BC film production and other gene synthesis processes.

The BC film produced by *Acetobacteraceae* has significant industrial applications. However, its nonessential production poses additional challenges for practical implementation<sup>[22]</sup>. Hence, there is a crucial need to design and develop genetic circuits for precise regulation of BC film production in *Acetobacteraceae*. Controlling the expression of genes related to BC production is a key way to precisely manage this process. Currently, the functions of several essential genes involved in cellulose production have been elu-

cidated. AcsA, a transmembrane protein, polymerizes UDP-glucose into  $\beta$ -1,4-glucan chains upon binding with the second messenger c-di-GMP. It perforates the bacterial inner membrane to allow glucan chain traversal<sup>[47–49]</sup>. AcsB, a periplasmic protein, stabilizes AcsA's catalytic activity<sup>[50]</sup> and guides glucan chains across the cytoplasm to the outer membrane<sup>[51]</sup>. The protein AcsC creates pores in the outer membrane to export glucan chains into the extracellular space. The protein CcpAX, a cellulose synthesis complementation factor, influences the expression of the AcsB and AcsC proteins and has been demonstrated to interact with AcsD. However, some homologous genes in the bacterial genome of *Acetobacteraceae* are not involved in BC production. Therefore, accurate identification of essential genes is necessary. In this study, cellulose production was analyzed in mutant strains lacking the *acsA*, *acsB*, *acsC*, and *dgc* (c-di-GMP synthase) homologous genes and the *ccpAX* gene. The four essential genes (*acsAB1*, *acsC1*, *ccpAX*, and *dgc2*) responsible for BC production in the *G. hansenii* ATCC 53582 strain were identified (Fig. 6c and d). This research provides a foundation and theoretical support for further design and regulation of cellulose film production in this strain.

## 5 Conclusions

This study focused on addressing the limited synthetic biology applications of *Acetobacteraceae* strains. First, by analyzing and evaluating three common BC-producing strains (*G. hansenii* ATCC 53582, *K. rhaeticus* iGEM, and *G. xylinus* 700178) for basic characteristics, such as cellulose film production, division time, antibiotic susceptibility, and plasmids, the strains *G. hansenii* ATCC 53582 and *K. rhaeticus* iGEM were found to be more suitable as host strains for engineering modifications. Two inducible promoters, pTrc and pLux101, were subsequently examined across the three strains. This study revealed that the inducibility of the pTrc promoter was relatively low among the three strains, whereas the pLux101 promoter exhibited significantly greater inducibility. Furthermore, gene knockout techniques confirmed the essentiality of four genes for BC film production in the genome of the *G. hansenii* ATCC 5358 strain. This research contributes to expanding the synthetic biology element library for nonmodel strains and lays the groundwork for the use of engineered *Acetobacteraceae* strains.

## Acknowledgements

The author thanks Dr. Tom Ellis from the Imperial College London for the *K. rhaeticus* iGEM strain and Dr. Siqian Chen from the Dongguan University of Technology for the *G. xylinus* 700178 strain.

## Conflict of interest

The authors declare that they have no conflict of interest.

## Biography

**Yanmei Gao** is a postdoctoral fellow at the University of Science and Technology of China. She received her Ph.D. degree from the University

of Science and Technology of China in 2023. Her research mainly focuses on bacterial gene circuits to design and program engineered bacteria for the treatment of wound infections.

## References

- [1] Rollié S, Mangold M, Sundmacher K. Designing biological systems: systems engineering meets synthetic biology. *Chemical Engineering Science*, **2012**, *69* (1): 1–29.
- [2] McNERNEY M P, DOIRON K E, NG T L, et al. Theranostic cells: emerging clinical applications of synthetic biology. *Nature Reviews: Genetics*, **2021**, *22*: 730–746.
- [3] Cameron D E, Bashor C J, Collins J J. A brief history of synthetic biology. *Nature Reviews Microbiology*, **2014**, *12*: 381–390.
- [4] Nora L C, Westmann C A, Guazzaroni M E, et al. Recent advances in plasmid-based tools for establishing novel microbial chassis. *Biotechnology Advances*, **2019**, *37* (8): 107433.
- [5] Mukherjee B, Madhu S, Wangikar P P. The role of systems biology in developing non-model cyanobacteria as hosts for chemical production. *Current Opinion in Biotechnology*, **2020**, *64*: 62–69.
- [6] Hwang S, Joung C, Kim W, et al. Recent advances in non-model bacterial chassis construction. *Current Opinion in Systems Biology*, **2023**, *36*: 100471.
- [7] Yan Q, Fong S S. Challenges and advances for genetic engineering of non-model bacteria and uses in consolidated bioprocessing. *Frontiers in Microbiology*, **2017**, *8*: 2060.
- [8] Riley L A, Guss A M. Approaches to genetic tool development for rapid domestication of non-model microorganisms. *Biotechnology for Biofuels*, **2021**, *14* (1): 30.
- [9] Mazzolini R, Rodríguez-Arce I, Fernández-Barat L, et al. Engineered live bacteria suppress *Pseudomonas aeruginosa* infection in mouse lung and dissolve endotracheal-tube biofilms. *Nature Biotechnology*, **2023**, *41*: 1089–1098.
- [10] Gilbert C, Tang T C, Ott W, et al. Living materials with programmable functionalities grown from engineered microbial cocultures. *Nature Materials*, **2021**, *20*: 691–700.
- [11] Cepec E, Trček J. Antimicrobial resistance of *Acetobacter* and *Komagataeibacter* species originating from vinegars. *International Journal of Environmental Research and Public Health*, **2022**, *19* (1): 463.
- [12] Mamlouk D, Gullo M. Acetic acid bacteria: physiology and carbon sources oxidation. *Indian Journal of Microbiology*, **2013**, *53*: 377–384.
- [13] Raspor P, Goranovič D. Biotechnological applications of acetic acid bacteria. *Critical Reviews in Biotechnology*, **2008**, *28* (2): 101–124.
- [14] Yamashita S, Oe M, Kimura M, et al. Improving effect of acetic acid bacteria (*Gluconacetobacter hansenii* GK-1) on slgA and physical conditions in healthy people: double-blinded placebo-controlled study. *Food and Nutrition Sciences*, **2022**, *13*: 541–557.
- [15] Sengun I Y, Karabiyikli S. Importance of acetic acid bacteria in food industry. *Food Control*, **2011**, *22* (5): 647–656.
- [16] Lynch K M, Zannini E, Wilkinson S, et al. Physiology of acetic acid bacteria and their role in vinegar and fermented beverages. *Comprehensive Reviews in Food Science and Food Safety*, **2019**, *18* (3): 587–625.
- [17] Moniri M, Boroumand Moghaddam A, Azizi S, et al. Production and status of bacterial cellulose in biomedical engineering. *Nanomaterials*, **2017**, *7* (9): 257.
- [18] Huang Y, Zhu C L, Yang J Z, et al. Recent advances in bacterial cellulose. *Cellulose*, **2014**, *21*: 1–30.
- [19] Srivastava S, Mathur G. Bacterial cellulose: a multipurpose biomaterial for manmade world. *Current Applied Science and Technology*, **2023**, *23* (3): 1–19.
- [20] Zheng L, Li S S, Luo J W, et al. Latest advances on bacterial cellulose-based antibacterial materials as wound dressings. *Frontiers in Bioengineering and Biotechnology*, **2020**, *8*: 593768.

- [21] Gorgieva S, Trček J. Bacterial cellulose: production, modification and perspectives in biomedical applications. *Nanomaterials*, **2019**, *9* (10): 1352.
- [22] Florea M, Hagemann H, Santosa G, et al. Engineering control of bacterial cellulose production using a genetic toolkit and a new cellulose-producing strain. *Proceedings of the National Academy of Sciences of the United States of America*, **2016**, *113* (24): E3431–E3440.
- [23] Liu L P, Yang X, Zhao X J, et al. A lambda red and FLP/FRT-mediated site-specific recombination system in *Komagataeibacter xylinus* and its application to enhance the productivity of bacterial cellulose. *ACS Synthetic Biology*, **2020**, *9* (11): 3171–3180.
- [24] Huang L H, Liu Q J, Sun X W, et al. Tailoring bacterial cellulose structure through CRISPR interference-mediated downregulation of galU in *Komagataeibacter xylinus* CGMCC 2955. *Biotechnology and Bioengineering*, **2020**, *117* (7): 2165–2176.
- [25] Jacek P, Kubiak K, Ryngajłło M, et al. Modification of bacterial nanocellulose properties through mutation of motility related genes in *Komagataeibacter hansenii* ATCC 53582. *New Biotechnology*, **2019**, *52*: 60–68.
- [26] Battad-Bernardo E, McCrindle S L, Couperwhite I, et al. Insertion of an *E. coli lacZ* gene in *Acetobacter xylinus* for the production of cellulose in whey. *FEMS Microbiology Letters*, **2004**, *231* (2): 253–260.
- [27] Hur D H, Choi W S, Kim T Y, et al. Enhanced production of bacterial cellulose in *Komagataeibacter xylinus* via tuning of biosynthesis genes with synthetic RBS. *Journal of Microbiology and Biotechnology*, **2020**, *30* (9): 1430–1435.
- [28] Mangayil R, Rajala S, Pammo A, et al. Engineering and characterization of bacterial nanocellulose films as low cost and flexible sensor material. *ACS Applied Materials & Interfaces*, **2017**, *9* (22): 19048–19056.
- [29] Fournet-Fayard S, Joly B, Forestier C. Transformation of wild type *Klebsiella pneumoniae* with plasmid DNA by electroporation. *Journal of Microbiological Methods*, **1995**, *24* (1): 49–54.
- [30] Taylor K, Woods S, Johns A, et al. Intrinsic responsible innovation in a synthetic biology research project. *New Genetics and Society*, **2023**, *42* (1): e2232684.
- [31] Carrillo Rincón A F, Farny N G. Unlocking the strength of inducible promoters in Gram-negative bacteria. *Microbial Biotechnology*, **2023**, *16* (5): 961–976.
- [32] Teh M Y, Ooi K H, Danny Teo S X, et al. An expanded synthetic biology toolkit for gene expression control in *Acetobacteraceae*. *ACS Synthetic Biology*, **2019**, *8* (4): 708–723.
- [33] Deng Y, Nagachar N, Xiao C, et al. Identification and characterization of non-cellulose-producing mutants of *Gluconacetobacter hansenii* generated by Tn5 transposon mutagenesis. *Journal of Bacteriology*, **2013**, *195* (22): 5072–5083.
- [34] Florea M, Reeve B, Abbott J, et al. Genome sequence and plasmid transformation of the model high-yield bacterial cellulose producer *Gluconacetobacter hansenii* ATCC 53582. *Scientific Reports*, **2016**, *6* (1): 23635.
- [35] Pfeiffer S, Mehta K, Brown Jr R M. Complete genome sequence of *Gluconacetobacter hansenii* strain NQ5 (ATCC 53582), an efficient producer of bacterial cellulose. *Genome Announcements*, **2016**, *4* (4): e00785–16.
- [36] Li F X, Ni L, Jin F. Development and application of a rapid gene manipulating toolbox for *Pseudomonas aeruginosa*. *Chinese Journal of Biotechnology*, **2023**, *39* (4): 1789–1803. (in Chinese)
- [37] Kim N M, Sinnott R W, Sandoval N R. Transcription factor-based biosensors and inducible systems in non-model bacteria: current progress and future directions. *Current Opinion in Biotechnology*, **2020**, *64*: 39–46.
- [38] Chen C T, Ding W X, Zhang H, et al. Bacterial cellulose-based biomaterials: From fabrication to application. *Carbohydrate Polymers*, **2022**, *278*: 118995.
- [39] Wünsche J, Schmid J. *Acetobacteraceae* as exopolysaccharide producers: Current state of knowledge and further perspectives. *Frontiers in Bioengineering and Biotechnology*, **2023**, *11*: 1166618.
- [40] Piraner D I, Abedi M H, Moser B A, et al. Tunable thermal bioswitches for in vivo control of microbial therapeutics. *Nature Chemical Biology*, **2017**, *13*: 75–80.
- [41] Chen Y H, Du M, Yuan Z, et al. Spatiotemporal control of engineered bacteria to express interferon- $\gamma$  by focused ultrasound for tumor immunotherapy. *Nature Communications*, **2022**, *13*: 4468.
- [42] Gao Y M, Wei J J, Pu L, et al. Remotely controllable engineered bacteria for targeted therapy of *Pseudomonas aeruginosa* infection. *ACS Synthetic Biology*, **2023**, *12* (7): 1961–1971.
- [43] Ohlendorf R, Vidavski R R, Eldar A, et al. From dusk till dawn: one-plasmid systems for light-regulated gene expression. *Journal of Molecular Biology*, **2012**, *416* (4): 534–542.
- [44] Lindner F, Diepold A. Optogenetics in bacteria – applications and opportunities. *FEMS Microbiology Reviews*, **2022**, *46* (2): fuab055.
- [45] Fu S W, Zhang R R, Gao Y M, et al. Programming the lifestyles of engineered bacteria for cancer therapy. *National Science Review*, **2023**, *10* (5): nwad031.
- [46] Chia N, Lee S Y, Tong Y. Optogenetic tools for microbial synthetic biology. *Biotechnology Advances*, **2022**, *59*: 107953.
- [47] Chien L J, Chen H T, Yang P F, et al. Enhancement of cellulose pellicle production by constitutively expressing *Vitreoscilla* hemoglobin in *Acetobacter xylinum*. *Biotechnology Progress*, **2006**, *22* (6): 1598–1603.
- [48] Ryjenkov D A, Simm R, Römling U, et al. The PilZ domain is a receptor for the second messenger c-di-GMP: the PilZ domain protein YcgR controls motility in enterobacteria. *Journal of Biological Chemistry*, **2006**, *281* (41): 30310–30314.
- [49] Morgan J L W, McNamara J T, Zimmer J. Mechanism of activation of bacterial cellulose synthase by cyclic di-GMP. *Nature Structural & Molecular Biology*, **2014**, *21*: 489–496.
- [50] Omadjela O, Narahari A, Strumillo J, et al. BcsA and BcsB form the catalytically active core of bacterial cellulose synthase sufficient for in vitro cellulose synthesis. *Proceedings of the National Academy of Sciences of the United States of America*, **2013**, *110* (44): 17856–17861.
- [51] Tajima K, Imai T, Yui T, et al. Cellulose-synthesizing machinery in bacteria. *Cellulose*, **2022**, *29*: 2755–2777.